Progress in Organic Coatings xxx (xxxx) xxxx

Contents lists available at ScienceDirect

Progress in Organic Coatings

journal homepage: www.elsevier.com/locate/porgcoat

Curing epoxy with ethylenediaminetetraacetic acid (EDTA) surface-functionalized $Co_xFe_{3-x}O_4$ magnetic nanoparticles

Maryam Jouyandeh[a], Mohammad Reza Ganjali[a,b,*], Jagar A. Ali[c], Mustafa Aghazadeh[a], Isa Karimzadeh[d], Krzysztof Formela[e], Xavier Colom[f], Javier Cañavate[f], Mohammad Reza Saeb[g,*]

[a] Center of Excellence in Electrochemistry, School of Chemistry, College of Science, University of Tehran, Tehran, Iran
[b] Biosensor Research Center, Endocrinology and Metabolism Molecular-Cellular Sciences Institute, Tehran University of Medical Sciences, Tehran, Iran
[c] Department of Petroleum Engineering, Faculty of Engineering, Soran University, Kurdistan Region, Iraq
[d] Department of Physics, Bonab Branch, Islamic Azad University, Bonab, Iran
[e] Department of Polymer Technology, Faculty of Chemistry, Gdańsk University of Technology, Gabriela Narutowicza 11/12, 80–233 Gdańsk, Poland
[f] Department of Chemical Engineering, Universitat Politècnica de Catalunya Barcelona Tech, Carrer de Colom, 1, 08222 Terrassa, Barcelona, Spain
[g] Department of Resin and Additives, Institute for Color Science and Technology, P.O. Box: 16765-654, Tehran, Iran

ARTICLE INFO

Keywords:
Cure Index
Epoxy
Fe_3O_4 nanoparticle
EDTA
Cobalt doping

ABSTRACT

In this work, the bulk and surface composition of Fe_3O_4 supermagnetic nanoparticles were modified for efficient epoxy curing. The bare, ethylenediaminetetraacetic acid (EDTA) capped, and cobalt (Co)-doped EDTA capped Fe_3O_4 nanoparticles were synthesized electrochemically. The crystalline structure and phase information, surface capping, morphology and magnetization behavior of nanoparticles were studied by X-Ray diffraction (XRD), Fourier-transform infrared spectroscopy (FTIR), field-emission scanning electron microscopy (FE-SEM) and vibrating sample magnetometer (VSM), respectively. A low amount of the prepared nanoparticle (0.1 wt.%) was used in preparation of epoxy nanocomposites. Nonisothermal differential scanning calorimetry (DSC) under different heating rates was performed to study the potential of nanoparticles in curing epoxy resin with an aliphatic amine. The heat release data on nanocomposites suggest that EDTA capped Co-doped Fe_3O_4 considerably improved the curing reaction between epoxy resin and the curing agent. Calculations based on *Cure Index* approved qualitatively a shift from *Poor* to *Good* cure by concurrent lattice and surface modifications of magnetic nanoparticles. It is bielived that the approach used in this work can pave the way to enhance curability of epoxy nanocomposites by the combined modification of bulk and surface of nanoparticles.

1. Introduction

Addition of nanoparticles and their surface functionalization has been practised over the past three decades in order to enhance the ultimate properties and performance of organic coatings [1–5]. A Nevertheless, there is a need for looking at properties of coatings containing functionalized nanoparticles from a molecular perspective so as to be able to tune properties by controlling the curability of thermoset resins under the influence of surface-functionalized nanoparticles. The difficulty is that no molecular-level gauge is available for quantifying the status quo of cross-link density of thermoset nanocomposite to assess whether or not functionalized nanoparticles added to the system are reactive towards curing moieties [6–8].

The effect of surface modification of a wide variety of nanoparticles with low- and high-molecular weight molecules of amine, carboxylic and hydroxyl on the curability of epoxy resin was addressed in previous works of this group, which are including carbon nanotubes (CNTs) [9–11], graphene oxide (GO) nanoflakes [12–14], halloysite nanotubes (HNTs) [15–17], silica nanoparticles [18,19] and zinc oxide (ZnO) nanoparticles [20]. Reports suggest that surface functionalization of nanoparticles with high-molecular-weight ethylenediaminetetraacetic acid (EDTA) can affect ultimate properties of cross-linkable polymer nanocomposites. For instance, Syuhada et al. showed that EDTA surface-functionalized GO was dispersed well in chitosan matrix due to interaction of EDTA functional groups with chitosan [21]. Well-dispersed GO-EDTA in chitosan matrix led to facilitation of stress transfer resulting in 71% improvement in tensile strength compared to the neat chitosan film.

Fe_3O_4 magnetic nanoparticles were found to be efficiently useful to improve corrosion inhibition and fire retardant properties of epoxy

* Corresponding author at: Center of Excellence in Electrochemistry, School of Chemistry, College of Science, University of Tehran, Tehran, Iran & Department of Resin and Additives, Institute for Color Science and Technology, P.O. Box: 16765-654, Tehran, Iran.
E-mail addresses: ganjali@ut.ac.ir (M.R. Ganjali), saeb-mr@icrc.ac.ir (M.R. Saeb).

https://doi.org/10.1016/j.porgcoat.2019.105248
Received 5 July 2019; Received in revised form 18 July 2019; Accepted 20 July 2019

nanocomposites [22]. Improved curability of epoxy/Fe_3O_4 nanocomposites under the influence of nanoparticle surface modification with acid [23], hydroxyl [24,25], and imide [26] was discussed in previous works of this group. It was also revealed that using *Cure Index* [27,28], *CI* criterion could be taken into account as a simple yet reliable procedure to to study curability of epoxy nanocomposites under non-isothermal differential scanning calorimetry (DSC), thereby to uncover the goodness of cure in terms of *Poor*, *Good*, and *Excellent* cure cases [15,19]. Nevertheless, effect of bulk composition or lattice manipulation of Fe_3O_4, alone or in combination with surface functionalization of Fe_3O_4 was not the subject of investigations.

In this work, the bulk and surface composition of Fe_3O_4 iron oxide nanoparticles (IONs) were respectively modified with cobalt (Co) and ethylenediaminetetraacetic acid (EDTA). The bare IONs, EDTA capped IONs (EDTA-IONs), and Co-doped EDTA-IONs were synthesized based on electrodeposition. The crystalline and phase structure of IONs and their surface characteristics were detected by X-Ray diffraction (XRD) and Fourier-transform infrared spectroscopy (FTIR) analyses, respectively. The morphology and magnetization behavior of nanoparticles were also studied by field-emission scanning electron microscopy (FE-SEM) and vibrating sample magnetometry (VSM), respectively. Low-filled epoxy nanocomposites containing 0.1 wt.% of three aforementioned types of IONs were prepared by mechanical and ultrasound-assisted mixing. Nonisothermal differential scanning calorimetry (DSC) measurements were performed to study the potential of nanoparticles in curing epoxy resin with an aliphatic amine. Eventually, nanocomposites were labeled for curability at diffeernt heating rates.

2. Experimental

2.1. Materials

Iron (III) nitrate nonahydrate (Fe $(NO_3)_3$. $6H_2O$), iron (II) chloride tetrachloride ($FeCl_2$. $4H_2O$), cobalt chloride hexahydrate ($CoCl_2$. $4H_2O$), and ethylenediaminetetraacetic acid disodium salt dehydrate (EDTA-Na_2, 99.9%) were purchased from Sigma-Aldrich and used without further modification. The graphite plates and stainless steel sheets (316 L) were provided from local companies. The epoxy resin (Epon-828) and triethylenetetramine (TETA) curing agent were provided by Hexion Co.

2.2. Synthesis of IONs samples

All the electrodeposition experiments were designed based on the cathodic electrodeposition *via*base generation strategy, previously reported[29–33]. The synthesis of bare IONs and EDTA coated IONs were repeated using the same procedure reported[32,33].The electrochemical cell was a stainless steel sheet centered between two graphite anodes, in which all electrodes were immerged into the electrolyte and connected to the external DC power supply by Cu wires. The applied experimental conditions were $i = 10\,mA\ cm^{-2}$, $t = 25\,min$ and pH = 6.5. In the deposition process of bare IONs, the electrolyte was 2 g iron(iii) nitrate + 1 g iron(ii) chloride dissolved the in one litter distilled H_2O. For deposition of EDTA coated IONs, only 1 g/L EDTA polymer as capping agent was added into the above-mentioned electrolyte. In the synthesis process of EDTA/Co-IONs, a simple aqueous electrolyte containing 1 g iron(II) chloride, 0.3 cobalt chloride, 2 g iron(III) nitrate and 1 g EDTA was used. After synthesis, the cathode electrodes were removed from the bath solutions i.e. electrolytes, and the deposited black films were separated from the electrode surfaces. Then these powders were washed several times with ethanol and heated at 70 °C for 2 h in vacuum oven. The final powders were used in the analyses tests. The schematic illustration of EDTA coated IONs is shown in Fig. 1.

2.3. Epoxy nanocomposites preparation

Four samples were prepared for further cure analysis: neat epoxy (EP), epoxy nanocomposite containing 0.1 wt.% bare IONs (EP/IONs), EDTA-IONs (EP/EDTA-IONs) and co-doped EDTA-IONs (EP/ Co-doped EDTA-IONs). By adding 0.1 wt.% of nanoparticles into epoxy resin and Sonicated with 50% duty cycle for 5 min, the epoxy nanocomposites will be prepared. After that, for getting well dispersal the nanocomposite blended with a mechanical mixer at 2500 rpm for 20 min. So as to study cure procedure of epoxy stoichiometric volume of TETA (100:13) was adjoined to epoxy system and combined completely.

2.4. Characterization

The crystalline nature and phase information of the prepared IONs powders were monitored by X-ray diffraction (XRD) conducted on a Phillips PW-1800 diffractometer. The patterns were provided by using Co-Kα radiation ($\lambda = 1.56$ Å) in the zone of $10^\circ < 2\theta < 80^\circ$ with steps of 0.015 and acquisition time of 2 s/step. The surface properties of nanoparticles was studied by a Bruker Vector 22 Fourier transform infrared (FT-IR) spectroscope. The IR spectra of samples were collected in the frequency range of 4000–400 cm^{-1} with resolution of 1.5 cm^{-1} to study if EDTA was successfully attached to the surface. The surface morphology observations were carried out by field-emission scanning electron microscopy (FE-SEM, Mira 3-XMU with accelerating voltage of 100 kV). The magnetization data were collected on Vibrating Sample Magnetometers (VSM, model Lakeshore 7410) at RT in the range of −20,000 to 20,000 Oe.

The curing state of epoxy resin and its nanocomposites consisted of 0.1 wt% EDTA-IONs and Co-doped EDTA-IONs was examined nanoisothermally on Perkin Elmer DSC 4000. Nonisothermal DSC was worked at heating degree (β) of 5, 10, 15, and 20 °C min^{-1} in the temperature range of 15–250 °C under nitrogen with the current speed of 20 mL.min^{-1}.

3. Results and discussion

3.1. Structural and microstructural analyses

The X-ray diffraction (XRD) patterns of the electro-deposited IONs powders were provided in Fig. 2. For all samples, well-defined diffractions of (111), (220), (311), (400), (422), (511), (440), (620) and (533) are specified in Fig. 2. These planes are well-fitted with those mentioned for Fe_3O_4 crystal phase of iron oxide (JCPDS No. 85-1436) [29–32,34]. The average crystallite sizes of bare IONs, ESTA/IONs and EDTA/Co-IONs samples were assessed using Debye Scherrer relation, i.e. $D = k\lambda/\beta\cos\theta$, where β is the full width of (311) plane at its half maximum (FWHM), λ is the X-ray beam wavelength ($\lambda_{Co} = 1.56$Å), θ is the Bragg angle for the actual peak and k is a shape function, where $k = 0.9$ was applied. The average crystalline sizes were 9.1 nm, 8.2 nm and 13.9 nm for bare IONs, EDTA/IONs and EDTA/Co-doped IONs, respectively.

FT-IR spectra of the fabricated Bare IONs, EDTA/IONs and EDTA/Co-doped IONs are presented in Fig. 3. In all spectra, the IR bands located at $\nu \leq 700\ cm^{-1}$ and 661 cm^{-1} are related to ν_1 and ν_2 vibration modes of the $Fe^{2+}-O^{2-}/Co^{2+}-O^{2-}$ and $Fe^{3+}-O^{2-}$ chemical bonds [29–32]. For EDTA capped IONs, various IR bands are observed in the wavenumbers of 700–1700 cm^{-1},; e.g. $\nu_{stretching}$ = 3280–3285 cm^{-1} for N−H bonds, $\nu_{stretching}$ = 2875–2880 cm^{-1} for N−C−H bonds, $\nu_{stretching}$ = 1625–1630 cm^{-1} for C=O groups, $\nu_{stretching}$ = 1475–1480 cm^{-1} for C−O bonds, $\nu_{wagging}$ = 1380–1385 cm^{-1} for CH_3 groups, $\nu_{stretching}$ = 1135–1140 cm^{-1} for C−N bonds and $\nu_{stretching}$ = 1025–1030 cm^{-1} for C−O−C bonds [29–33], where these IR bands confirmed the attachment of EDTA layer onto the surface of the electrodeposited IONs particles.

Surface morphology of the prepared IONs was characterized by FE-

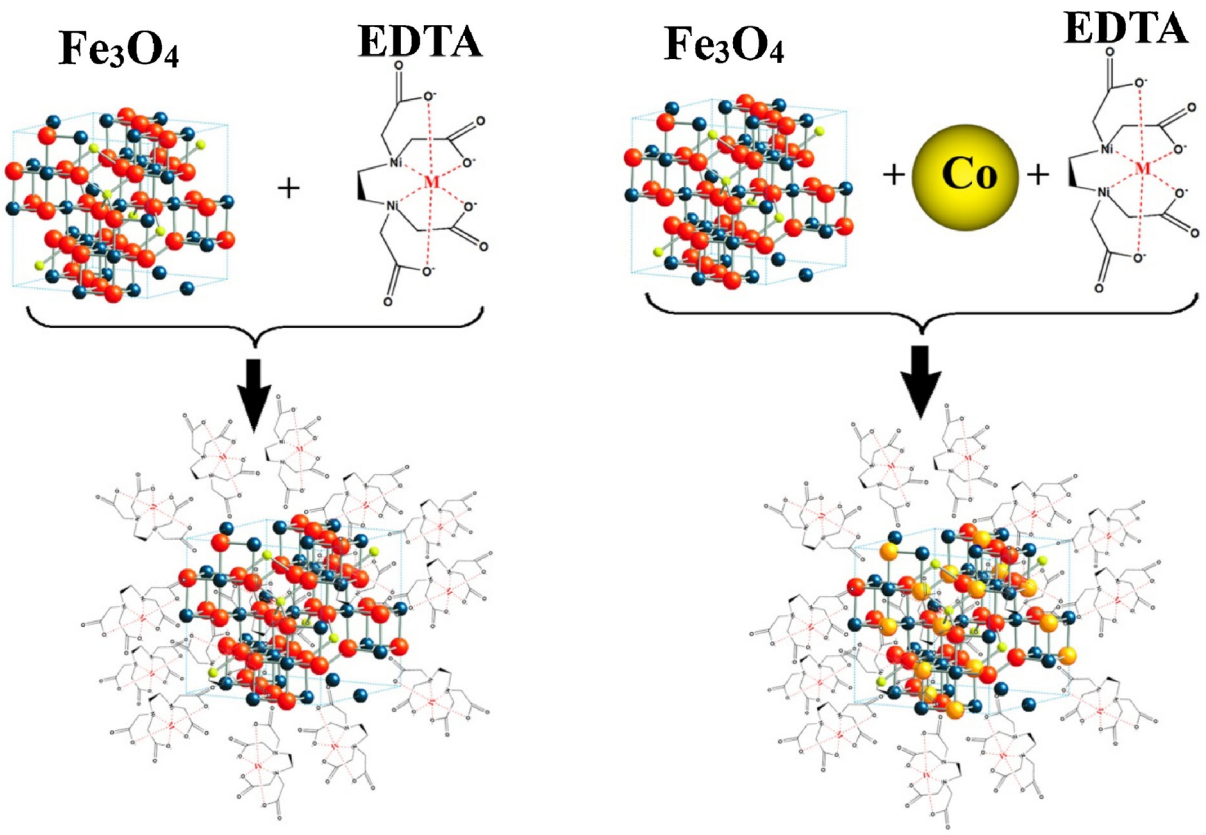

Fig. 1. EDTA coating of Fe_3O_4 and Co-doped Fe_3O_4.

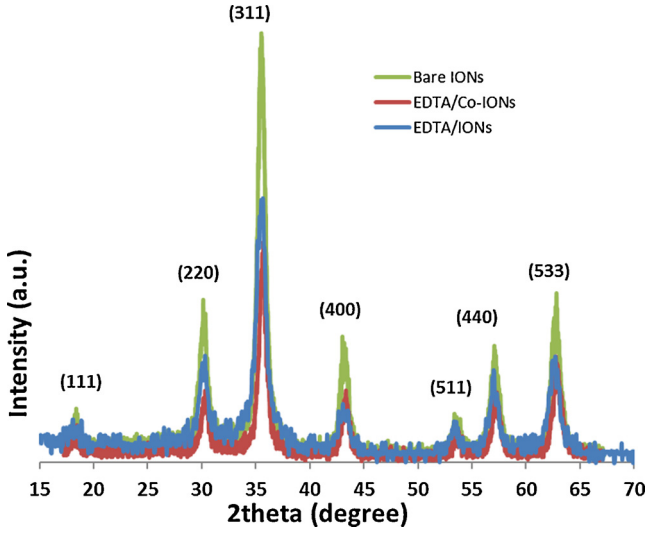

Fig. 2. XRD patterns of the synthesized bare IONs [32], EDTA/ IONs [33] and EDTA/Co-doped IONs.

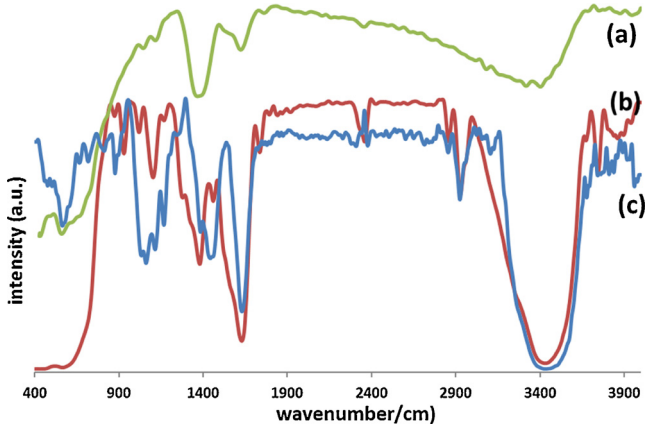

Fig. 3. FT-IR spectra of the synthesized (a) bare IONs [32], (b) EDTA/IONs [33] and (c) EDTA/Co-doped IONs.

SEM micrographs (Fig. 4). It is clearthat all the deposited IONs samples have spherical particles. The average diameters of 20 nm, 40 nm and 35 nm were measured for bare IONs, EDTA/IONs and EDTA/Co-doped IONs, respectively (Fig. 4).

Fig. 5 shows the VSM plots for the prepared IONPs particles. The VSM profiles of all three IONs exhibited a complete S shape, indicative of their superparamagnetic behavior. From Fig. 5, the saturation magnetization (*Ms*), remanence (*Mr*) and coercivity (*Hci*) values were extracted to be *Ms* = 72.96 emu/g, *Mr* = 0.82 emu/g and *Hci* = 2.9 Oe for the bare IONsm which is in accordance with a previous report [32], while *Ms* = 51.89 emu/g, *Mr* = 0.59 emu/g and *Hci* = 0.85 Oe we extracted for EDTA-IONs as reported in a previous study [33]. Moreover, *Ms* = 33.68 emu/g, *Mr* = 0.72 emu/g and *Hci* = 1.04 Oe were assigned to EDTA/Co-IONs. The low H_{Ci} and negligible *Mr* for all three fabricated IONs proved their superparamagnetic properties. These data indicated that the magnetization of IONs is reduced as a result of surface coating with EDTA, and Co^{2+}-doping into their crystalline zones, which was due to the reduction in magnetite fraction of the samples. The low values measured for the *Hci* and *Mr* quantities indicated an improvement in the superparamagnetic performances of both EDTA-coated IONs and Co-doped EDTA-IONs sample as compared with bare IONs.

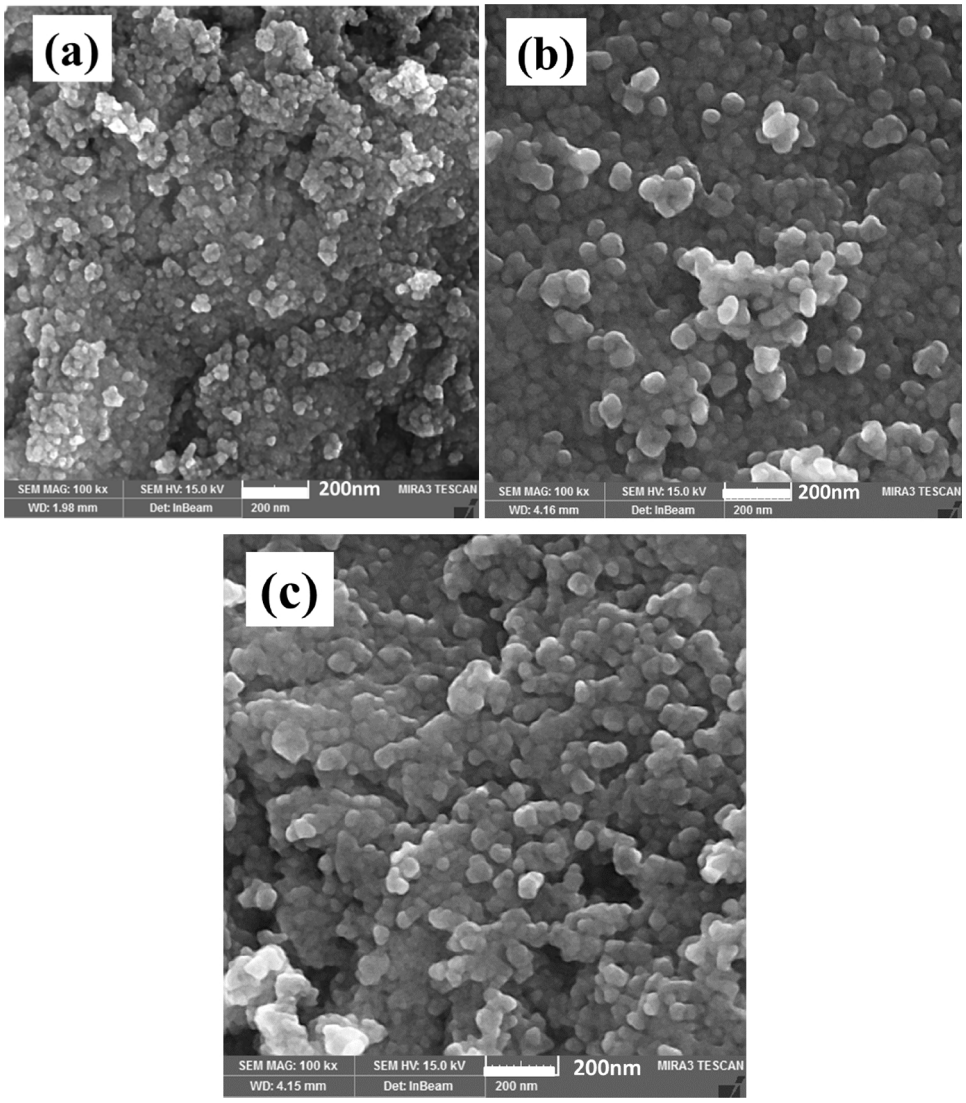

Fig. 4. FE-SEM images of bare IONs [32], (b) EDTA/ IONs and (c) EDTA/Co-doped IONs.

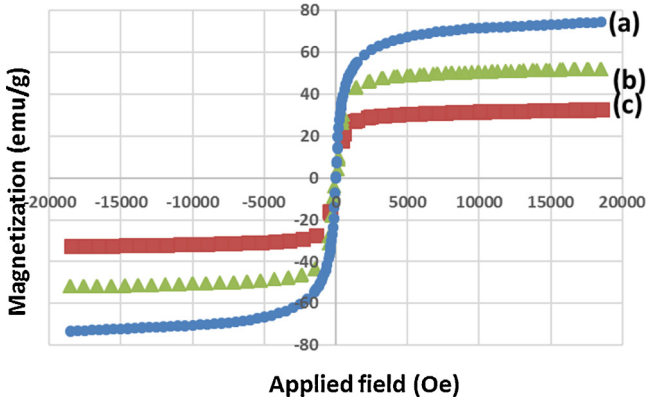

Fig. 5. VSM curves of the fabricated (a) bare IONs, (b) EDTA/ IONs and (c) EDTA/Co-doped IONs.

3.2. Cure analysis

The cure curves that achieved based on nonisothermal DSC at β of 5, 10, 15 and 20 °C/min are shown and compared in Fig. 6. The exothermic peaks in all the samples at four heating rates are signature of occurance of epoxy ring opening with amine groups of curing agent as the dominant event taking place in the system [35].

Cure states of epoxy composites containing EDTA coated and Co-doped IONs were studied qualitatively by *the CI* based on non-osothermal cure protocol proposed for thermoset systems [28]. the dimensionless *CI*was calculated as follows:

$$\Delta H^* = \frac{\Delta H_C}{\Delta H_{\mathrm{Ref}}} \quad (1)$$

$$\Delta T^* = \frac{\Delta T_C}{\Delta T_{\mathrm{Ref}}} \quad (2)$$

$$CI = \Delta H^* \times \Delta T^* \quad (3)$$

ΔH_C, ΔT_C and ΔH_{Ref}, ΔT_{Ref} are the heat released during the whole cure process, temperature interval for epoxy nanocomposite, and in the same order for blank epoxy, respectively.

The values of ΔT^*, ΔH^* and the *CI* for EP/IONs, EP/EDTA-IONs and EP/Co-doped EDTA-IONs nanocomposites at different heating rates of 5, 10, 15 and 20 °C/min are presented in Table 1. The onset and endset cure temperature (T_{onset} and T_{endset}), total temperature interval (ΔT), the maximum temperature of DSC curve (T_p) and total enthalpy of cure (ΔH_∞) are also reported in Table 1.

According to Table 1, by addition of nanoparticles the value of T_{onset} increased compared to that of neat epoxy due to the steric hindrance

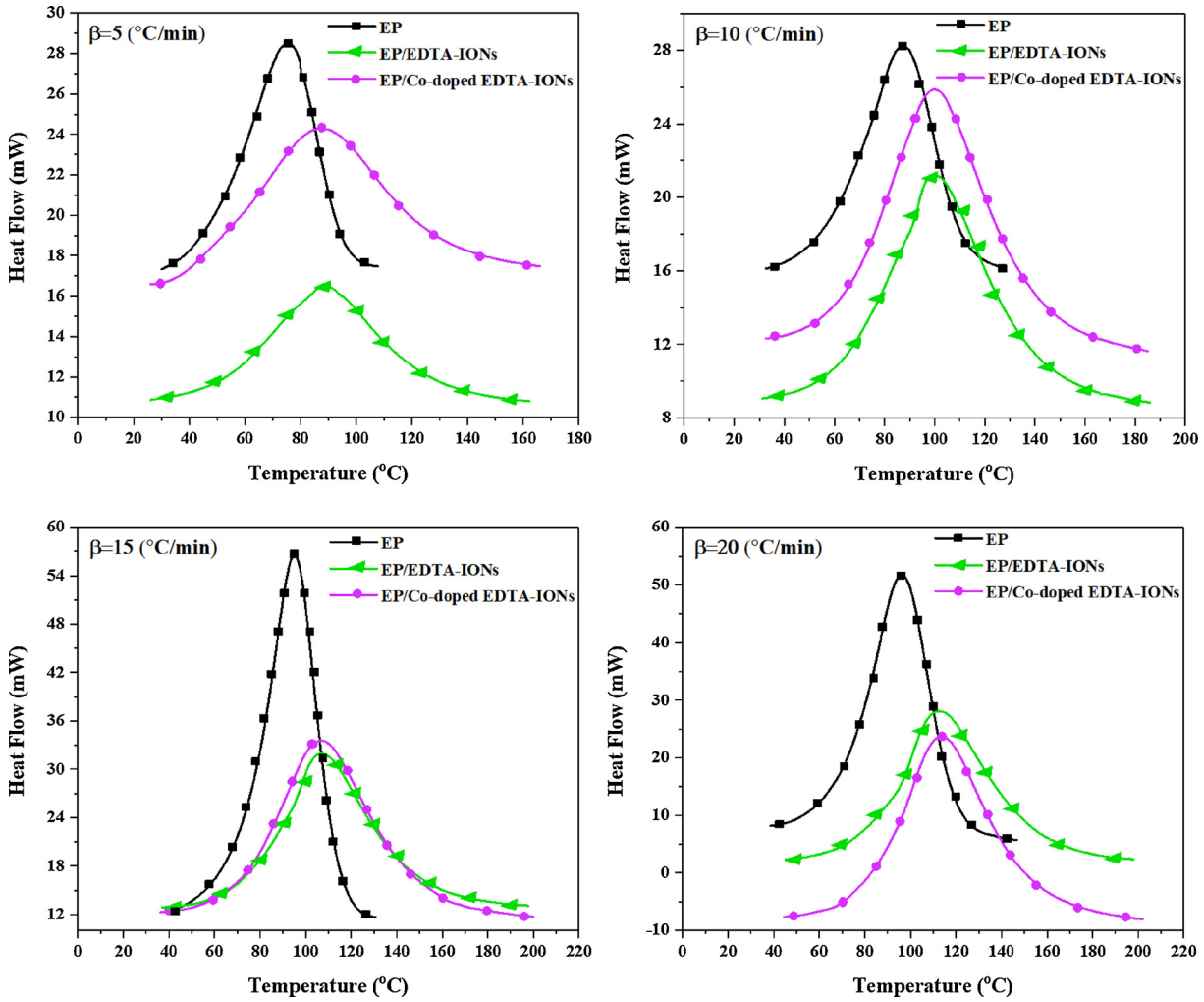

Fig. 6. Dynamic DSC thermograms of EP, EP/EDTA-IONs and EP/Co-doped EDTA-IONs at different heating rates.

effect brough about by nanoparticles[36]. In the case of EDTA-IONs and Co-doped EDTA-IONs incorporated epoxy systems, the presence of EDTA with COOH groups significantly increased the total time of cure. Moreover, EDTA attached to the surface of EDTA-IONs and Co-doped EDTA-IONs also improved ΔH_∞ values compared to EP/IONs, which indicates formation of denser cross-linked networks [37].

As can be recognized by looking at data in Table 1, addition of pristine IONs hindered curing reaction of epoxy. On the other hand, surface functionalization of IONs nanoparticles by EDTA was the reason respectively for lower and higher T_{onset} and T_{endset} values at all heating rates with respect to EP/IONs. It means that the reaction of EDTA on the surface of IONs with epoxide ring enlarged cure temperature interval. At the same time, ΔH_∞ increased due to the reaction of carboxyl groups of EDTA with epoxide groups of resin, but still the amount of its heat release is lower than that of neat epoxy. On the other hand, EDTA coated Co-doped IONs nanoparticles were apparently able to increase ΔH_∞ of cure compared to the neat epoxy and its nanocomposites containing pristine and EDTA-functionalized IONs nanoparticles. The COOH groups of EDTA on the surface of Co-doped IONs nanoparticles participated in epoxide ring opening and facilitated curing reaction (Fig. 7). The main reaction taking place between COOH and epoxy yields β-hydroxypropyl ester, which is responsible for reaction with a second COOH group at high temperature to yield a diester. This cross-linking reaction can occur at lower temperatures with the use of tertiary amines as catalyst [38]. Since the COOH groups is in the second priority in comparison with amine groups of curing agent in epoxide ring opening, the total temperature of cure increased because of the fact that their nucleophilicity was much lower than the above-mentioned amine-containing curing agents [39].

Fig. 8 gives a general view to understand the role of nanoparticles in epoxy crosslinking. In the Fig. 8 the green area is *Excellent* cure region ($\Delta T^* < CI < \Delta H^*$), the blue area *Good* cure zone ($CI > \Delta H^*$) and the red area *Poor* cure in which EDTA-coated and Co-doped IONs nanoparticles existed in epoxy ($CI < \Delta T^*$).

As shown in Fig. 8, at low heating rates (β = 5 and 10 °C/min) the reaction is slow and curing moieties, and COOH groups of EDTA on the surface of Co-doped IONs nanoparticles, have enough time to participate in curing reaction of epoxy leading to the *CI* values higher than ΔH^* (*Good* cure state). On the other hand, at high β (20 °C/min) the reaction time was low, but kinetic energy per molecules was high enough to increase the curing reaction leading to to *Good* cure state. Thus, engineering of the surface of nanoparticles changed cure label of epoxy.

4. Conclusion

Pristine,EDTA coated and Co^{2+} doped IONs nanoparticles were prepared through cathodic electrodeposition *via*base generation strategy. The crystalline nature and phase information of the pristine IONs and EDTA-coated IONs and Co^{2+}-doped IONs powders were studied by XRD analysis. From Debye Scherrer relation and using XRD data the average crystalline size of bare IONs, EDTA/IONs and EDTA/Co-doped IONs were calculated to be 9.1 nm, 8.2 nm and 13.9 nm, respectively. The surface functionalization was confirmed by FT-IR. FESEM images confirmed the average diameters of 20 nm, 40 nm and

Table 1
Cure characteristics of the prepared epoxy nanocomposites as a function of heating rate.

Designation	β(°C/min)	T_{onset}(°C)	T_{endset}(°C)	T_p(°C)	ΔT(°C)	ΔH_∞(J/g)	ΔT*	ΔH*	CI
EP	5	30.04	107.62	75.31	77.58	340.41	n.a.	n.a.	n.a.
	10	29.7	165.3	98.4	135.7	319.4	n.a.	n.a.	n.a.
	15	36.64	191.89	107.89	155.25	377.61	n.a.	n.a.	n.a.
	20	38.62	146.67	96.09	108.05	374.39	n.a.	n.a.	n.a.
EP/IONs	5	40.7	140.4	90.3	99.6	186.6	0.83	0.55	0.45
	10	40.7	166.0	99.1	125.3	310.8	0.92	0.97	0.90
	15	46.1	174.4	113.0	128.3	127.7	0.83	0.34	0.28
	20	46.9	191.5	118.0	144.7	164.3	0.90	0.44	0.40
EP/EDTA-IONs	5	26.05	162.14	88.78	136.09	277.46	1.75	0.81	1.42
	10	31.11	285.95	100.3	154.84	306.07	1.14	0.96	1.09
	15	37.03	197.78	106.90	160.75	310.28	1.03	0.82	0.84
	20	45.20	197.88	112.69	152.68	315.41	1.41	0.84	1.18
EP/Co-doped EDTA-IONs	5	26.12	165.94	87.55	139.82	416.96	1.80	1.22	2.19
	10	32.61	184.96	100.02	152.35	352.29	1.12	1.10	1.24
	15	36.19	199.95	106.76	163.76	375.35	1.05	0.99	1.04
	20	45.54	201.90	114.59	156.35	389.45	1.45	1.04	1.51
n.a. – not applicable (reference measurements)									

n.a. - not applicable (reference measurements).

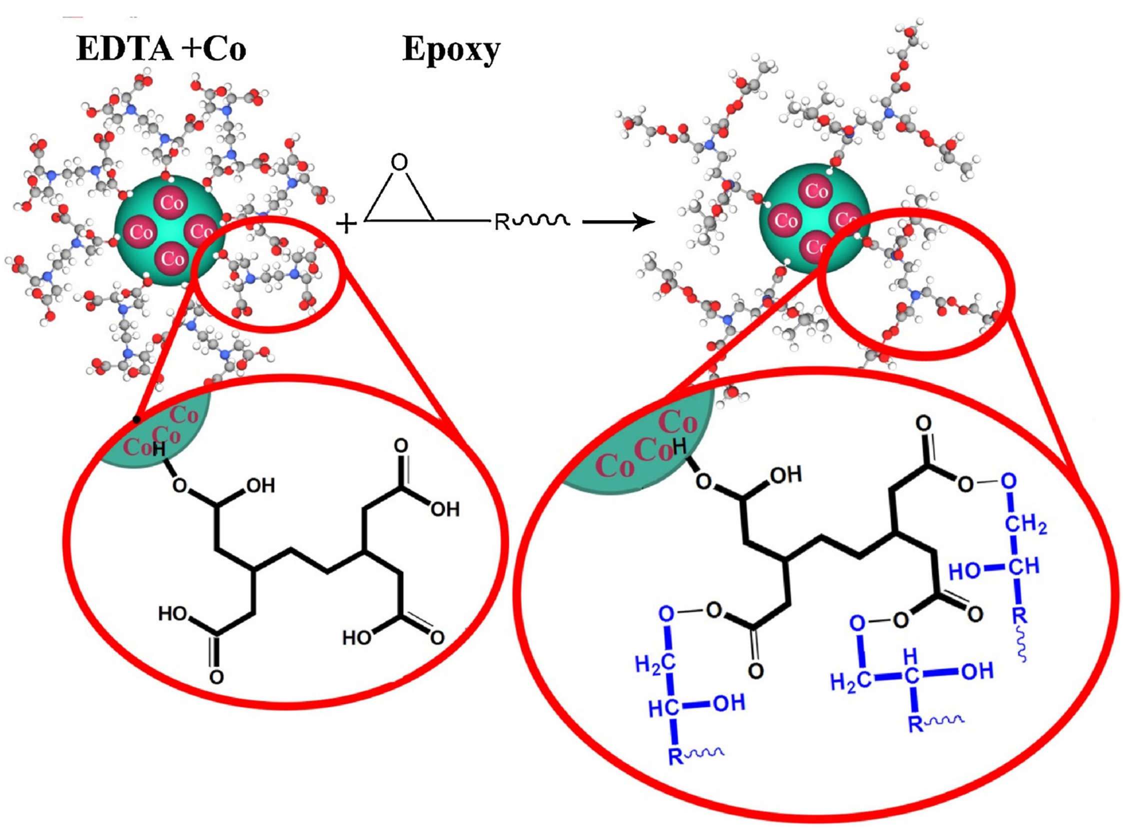

Fig. 7. Reaction between EDTA on the surface of Co-doped IONs and epoxy.

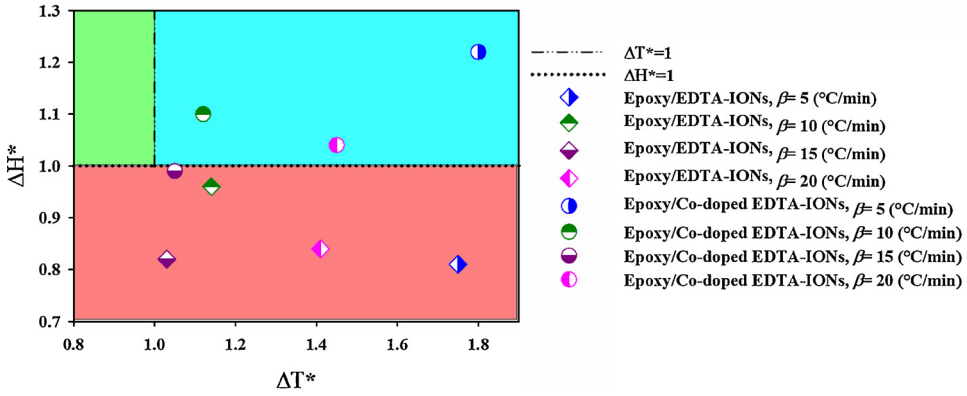

Fig. 8. Cure state of EP/EDTA-IONs and EP/Co-doped EDTA-IONs nanocomposites at heating rates of 5, 10, 15 and 20 °C/min.

35 nm for pristine IONs, EDTA-coated IONs and Co^{2+} doped IONs, respectively. The potential of the prepared nanoparticles for cure reaction of epoxy resin at low level of particles (0.1 wt.%) was investigated by nonisothermal DSC at heating rates of 5, 10, 15 and 20 °C/min. DSC results showed that pristine IONs hindered epoxy curing reaction with amine hardener as reflected in a significant drop in ΔH_∞ values even more than 50% ($\Delta H^* = 0.34$ at $\beta = 15$ °C/min). By contrast, EDTA-capped IONs increased ΔH_∞ compared to the bare IONs at all heating rates. The value of ΔH_∞ significantly increased from 127 J/g for EP/IONs to 310 J/g for EP/EDTA-IONs. Catalyzing effect of COOH of EDTA and Co^{2+} in the lattice of IONs led to change in cure label of epoxy/amine system from *Poor* to *Good* at $\beta = 5$, 10 and 20 °C/min.

References

[1] M. Aliakbari, O.M. Jazani, M. Sohrabian, M. Jouyandeh, M.R. Saeb, Multi-nationality epoxy adhesives on trial for future nanocomposite developments, Prog. Org. Coat. 133 (2019) 376–386.
[2] Z. Ahmadi, Epoxy in nanotechnology: a short review, Prog. Org. Coat. 132 (2019) 445–448.
[3] M.R. Saeb, H. Vahabi, M. Jouyandeh, E. Movahedifar, R. Khalili, Epoxy-based flame retardant nanocomposite coatings: comparison between functions of expandable graphite and halloysite nanotubes, Prog. Color Colorants Coat. 10 (2017) 245–252.
[4] M. Jouyandeh, O. Jazani, A. Navarchian, M.R. Saeb, Epoxy coatings physically cured with hydroxyl-contained silica nanospheres and halloysite nanotubes, progress in color, Colorants Coat. 11 (2018) 199–207.
[5] Z. Karami, O.M. Jazani, A. Navarchian, M.R. Saeb, Effect of carbon black content on curing behavior of Polysulfide Elastomer, Prog. Color Colorants Coat. 12 (2018) 103–112.
[6] T.A. Truc, T.T. Thuy, V.K. Oanh, T.T.X. Hang, A.S. Nguyen, N. Caussé, N. Pébère, 8-hydroxyquinoline-modified clay incorporated in an epoxy coating for the corrosion protection of carbon steel, Surf. Interfaces 14 (2019) 26–33.
[7] Y. Situ, W. Ji, C. Liu, J. Xu, H. Huang, Synergistic effect of homogeneously dispersed PANI-TiN nanocomposites towards long-term anticorrosive performance of epoxy coatings, Prog. Org. Coat. 130 (2019) 158–167.
[8] R. Sun, L. Li, C. Feng, S. Kitipornchai, J. Yang, Tensile property enhancement of defective graphene/epoxy nanocomposite by hydrogen functionalization, Compos. Struct. (2019) 111079.
[9] M.R. Saeb, E. Bakhshandeh, H.A. Khonakdar, E. Mäder, C. Scheffler, G. Heinrich, Cure kinetics of epoxy nanocomposites affected by MWCNTs functionalization: a review, Transfus. Apher. Sci. 2013 (2013).
[10] M.R. Saeb, F. Najafi, E. Bakhshandeh, H.A. Khonakdar, M. Mostafaiyan, F. Simon, C. Scheffler, E. Mäder, Highly curable epoxy/MWCNTs nanocomposites: an effective approach to functionalization of carbon nanotubes, Chem. Eng. J. 259 (2015) 117–125.
[11] M.R. Saeb, H. Rastin, M. Nonahal, M. Ghaffari, A. Jannesari, K. Formela, Cure kinetics of epoxy/MWCNTs nanocomposites: nonisothermal calorimetric and rheokinetic techniques, J. Appl. Polym. Sci. 134 (2017) 45221.
[12] M. Nonahal, H. Rastin, M.R. Saeb, M.G. Sari, M.H. Moghadam, P. Zarrintaj, B. Ramezanzadeh, Epoxy/PAMAM dendrimer-modified graphene oxide nanocomposite coatings: nonisothermal cure kinetics study, Prog. Org. Coat. 114 (2018) 233–243.
[13] E. Yarahmadi, K. Didehban, M.G. Sari, M.R. Saeb, M. Shabanian, F. Aryanasab, P. Zarrintaj, S.M.R. Paran, M. Mozafari, M. Rallini, Development and curing potential of epoxy/starch-functionalized graphene oxide nanocomposite coatings, Prog. Org. Coat. 119 (2018) 194–202.
[14] M. Nonahal, M.R. Saeb, S. Hassan Jafari, H. Rastin, H.A. Khonakdar, F. Najafi, F. Simon, Design, preparation, and characterization of fast cure epoxy/amine-functionalized graphene oxide nanocomposites, Polym. Compos. 39 (2018) E2016–E2027.
[15] M. Jouyandeh, O.M. Jazani, A.H. Navarchian, M. Shabanian, H. Vahabi, M.R. Saeb, Bushy-surface hybrid nanoparticles for developing epoxy superadhesives, Appl. Surf. Sci. 479 (2019) 1148–1160.
[16] M. Jouyandeh, Z. Karami, O. Moini Jazani, K. Formela, S.M.R. Paran, A. Jannesari, M.R. Saeb, Curing epoxy resin with anhydride in the presence of halloysite nanotubes: the contradictory effects of filler concentration, Prog. Org. Coat. 126 (2019) 129–135.
[17] V. Akbari, F. Najafi, H. Vahabi, M. Jouyandeh, M. Badawi, S. Morisset, M.R. Ganjali, M.R. Saeb, Surface chemistry of halloysite nanotubes controls the curability of low filled epoxy nanocomposites, Prog. Org. Coat. 135 (2019) 555–564.
[18] M. Jouyandeh, O.M. Jazani, A.H. Navarchian, M. Shabanian, H. Vahabi, M.R. Saeb, Surface engineering of nanoparticles with macromolecules for epoxy curing: development of super-reactive nitrogen-rich nanosilica through surface chemistry manipulation, Appl. Surf. Sci. 447 (2018) 152–164.
[19] F. Tikhani, M. Jouyandeh, S.H. Jafari, S. Chabokrow, M. Ghahari, K. Gharanjig, F. Klein, N. Hampp, M.R. Ganjali, K. Formela, M.R. Saeb, Cure Index demonstrates curing of epoxy composites containing silica nanoparticles of variable morphology and porosity, Prog. Org. Coat. 135 (2019) 176–184.
[20] M.G. Sari, M.R. Saeb, M. Shabanian, M. Khaleghi, H. Vahabi, C. Vagner, P. Zarrintaj, R. Khalili, S.M.R. Paran, B. Ramezanzadeh, Epoxy/starch-modified nano-zinc oxide transparent nanocomposite coatings: a showcase of superior curing behavior, Prog. Org. Coat. 115 (2018) 143–150.
[21] N. Syuhada, N. Huang, S. Vijay Kumar, H. Lim, S. Rahman, G. Thien, N. Ibrahim, M. Ahmad, P. Moradihamedani, Enhanced mechanical properties of chitosan/EDTA-GO nanocomposites thin films, Sains Malaysiana 43 (2014) 851–859.
[22] M. Jouyandeh, N. Rahmati, E. Movahedifar, B.S. Hadavand, Z. Karami, M. Ghaffari, P. Taheri, E. Bakhshandeh, H. Vahabi,, M.R. Ganjaliaj, K. Formelak, M.R. Saebabchi, Properties of nano-Fe_3O_4 incorporated epoxy coatings from Cure Index perspective, Prog. Org. Coat. 133 (2019) 220–228.
[23] M. Jouyandeh, M. Shabanian, M. Khaleghi, S.M.R. Paran, S. Ghiyasi, H. Vahabi, K. Formela, D. Puglia, M.R. Saeb, Acid-aided epoxy-amine curing reaction as reflected in epoxy/Fe3O4 nanocomposites: chemistry, mechanism, and fracture behavior, Prog. Org. Coat. 125 (2018) 384–392.
[24] M.R. Saeb, M. Nonahal, H. Rastin, M. Shabanian, M. Ghaffari, G. Bahlakeh, S. Ghiyasi, H.A. Khonakdar, V. Goodarzi, P. Vijayan, D. Puglia, Calorimetric analysis and molecular dynamics simulation of cure kinetics of epoxy/chitosan-modified Fe_3O_4 nanocomposites, Prog. Org. Coat. 112 (2017) 176–186.
[25] M.R. Saeb, H. Rastin, M. Shabanian, M. Ghaffari, G. Bahlakeh, Cure kinetics of epoxy/β-cyclodextrin-functionalized Fe_3O_4 nanocomposites: experimental analysis, mathematical modeling, and molecular dynamics simulation, Prog. Org. Coat. 110 (2017) 172–181.
[26] M. Jouyandeh, S.M.R. Paran, M. Shabanian, S. Ghiyasi, H. Vahabi, M. Badawi, K. Formela, D. Puglia, M.R. Saeb, Curing behavior of epoxy/Fe_3 O_4 nanocomposites: a comparison between the effects of bare Fe_3 O_4, Fe_3 O_4/SiO_2/chitosan and Fe_3 O_4/SiO_2/chitosan/imide/phenylalanine-modified nanofillers, Prog. Org. Coat. 123 (2018) 10–19.
[27] M. Jouyandeh, S.M.R. Paran, A. Jannesari, M.R. Saeb, 'Cure Index' for thermoset composites, Prog. Org. Coat. 127 (2019) 429–434.
[28] M. Jouyandeh, S.M.R. Paran, A. Jannesari, D. Puglia, M.R. Saeb, Protocol for nonisothermal cure analysis of thermoset composites, Prog. Org. Coat. 131 (2019) 333–339.
[29] M. Aghazadeh, I. Karimzadeh, M.R. Ganjali, A. Malekinezhad, Al^{3+} doped Fe_3O_4 nanoparticles: a novel preparation method, structural, magnetic and electrochemical characterizations, Int. J. Electrochem. Sci. 12 (2017) 8033–8044.
[30] M. Aghazadeh, I. Karimzadeh, M.R. Ganjali, PVP capped Mn_2+ doped Fe_3O_4 nanoparticles: a novel preparation method, surface engineering and characterization, Mater. Lett. 228 (2018) 137–140.
[31] I. Karimzadeh, M. Aghazadeh, M.R. Ganjali, P. Norouzi, S. Shirvani-Arani, T. Doroudi, P.H. Kolivand, S.A. Marashi, D. Gharailou, A novel method for preparation of bare and poly (vinylpyrrolidone) coated superparamagnetic iron oxide nanoparticles for biomedical applications, Mater. Lett. 179 (2016) 5–8.
[32] M. Aghazadeh, Zn-doped magnetite nanoparticles: development of novel preparation method and evaluation of magnetic and electrochemical capacitance

performances, J. Mater. Sci. Mater. Electron. 28 (2017) 18755–18764.
[33] M. Aghazadeh, I. Karimzadeh, M.R. Ganjali, Ethylenediaminetetraacetic acid capped superparamagnetic iron oxide (Fe_3O_4) nanoparticles: a novel preparation method and characterization, J. Magn. Magn. Mater. 439 (2017) 312–319.
[34] M. Aghazadeh, I. Karimzadeh, M.R. Ganjali, M.G. Maragheh, Electrochemical fabrication of praseodymium cations doped iron oxide nanoparticles with enhanced charge storage and magnetic capabilities, J. Mater. Sci. Mater. Electron. 29 (2018) 5163–5172.
[35] S. Ghiyasi, M.G. Sari, M. Shabanian, M. Hajibeygi, P. Zarrintaj, M. Rallini, L. Torre, D. Puglia, H. Vahabi,, M. Jouyandeh, F. Laoutid, S.M.Reza. Paran and M.R. Saeb,, Hyperbranched poly (ethyleneimine) physically attached to silica nanoparticles to facilitate curing of epoxy nanocomposite coatings, Prog. Org. Coat. 120 (2018) 100–109.
[36] A. Kondyurin, L.A. Komar, A.L. Svistkov, Combinatory model of curing process in epoxy composite, Compos. Part B Eng. 43 (2012) 616–620.
[37] C. Lou, X. Liu, Functional dendritic curing agent for epoxy resin: processing, mechanical performance and curing/toughening mechanism, Compos. Part B Eng. 136 (2018) 20–27.
[38] U.Q. Ly, M.-P. Pham, M.J. Marks, T.N. Truong, Density functional theory study of mechanism of epoxy-carboxylic acid curing reaction, J. Comput. Chem. 38 (2017) 1093–1102.
[39] T. Vidil, F. Tournilhac, S. Musso, A. Robisson, L. Leibler, Control of reactions and network structures of epoxy thermosets, Prog. Polym. Sci. 62 (2016) 126–179.